Polarized spectral properties and laser operation of Nd:SrAl12O19 crystal

Yuxin Pan, Bei Liu, Jian Liu, Qingsong Song, Jie Xu, Dongzhen Li, Peng Liu, Jie Ma, Xiaodong Xu, Hui Lin, et al.

Polarized spectral properties and laser operation of Nd:$SrAl_{12}O_{19}$ crystal

YUXIN PAN,[1,2] BEI LIU,[1] JIAN LIU,[3] QINGSONG SONG,[1] JIE XU,[1] DONGZHEN LI,[1] PENG LIU,[1] JIE MA,[1] XIAODONG XU,[1,5] HUI LIN,[2] JUN XU,[3,6] AND KHEIRREDDINE LEBBOU[4]

[1]*Jiangsu Key Laboratory of Advanced Laser Materials and Devices, School of Physics and Electronic Engineering, Jiangsu Normal University, Xuzhou 221116, China*
[2]*Engineering Research Center of Optical Instrument and System, Ministry of Education and Shanghai Key Lab of Modern Optics and Systems, University of Shanghai for Science and Technology, 200093, China*
[3]*School of Physics Science and Engineering, Institute for Advanced Study, Tongji University, Shanghai 200092, China*
[4]*Institut Lumière Matière, UMR5306 Université Lyon1-CNRS, Université de Lyon, Lyon 69622, Villeurbanne Cedex, France*
[5]*xdxu79@jsnu.edu.cn*
[6]*xujun@mail.shcnc.ac.cn*

Abstract: Nd:$SrAl_{11}O_{19}$ (Nd:SRA) crystal has been grown by the Czochralski method. Polarized absorption spectra, polarized fluorescence spectra and fluorescence lifetime were investigated. For σ-polarization, the peak absorption cross section at 798 nm is 2.08×10^{-20} cm^2 with full width at half maximum (FWHM) of 10.2 nm and the peak emission cross section is 3.36×10^{-20} cm^2 at 1048.5 nm with FWHM of 4.80 nm. The Judd-Ofelt parameters $\Omega_{2,4,6}$ were obtained to be 0.51×10^{-20} cm^2, 2.08×10^{-20} cm^2, and 2.12×10^{-20} cm^2, respectively. Continuous-wave laser operation of the a-cut and c-cut Nd:SRA sample has been demonstrated. The maximum output power of 8.33 W was achieved from c-cut sample at an absorbed power of 27.73 W, corresponding to a slope efficiency of 31.3%.

Key words: Nd:SRA; Czochralski method; Judd-Ofelt theory; Continuous-wave laser

1. Introduction

Laser sources operating at 1.0 μm wavelength region have attracted much attention due to their important applications, such as biology, medical detection, optical communication and scientific research [1-3]. In general, 1.0 μm wavelength laser was realized in trivalent Yb^{3+}- and Nd^{3+}-doped laser materials. Compared with Yb^{3+}-doped gain materials, Nd^{3+}-doped materials have relatively large emission cross section and negligible re-absorption loss due to their four-level operation. Among Nd^{3+}-doped laser crystals, Nd:YAG crystal has been proved to be excellent materials because of good physical and chemical properties. However, Nd:YAG crystal is limited to low Nd^{3+} doping concentration, narrow absorption and emission bandwidth, which causes a strong sensitivity to the pumping wavelength of AlGaAs laser diodes and limits the pulse width when used for mode-locked lasers. Nd^{3+}-doped disordered crystals are promising in realizing mode-locked femtosecond laser, because they possess better thermal conductivity than Nd:glass and broader emission spectra than Nd:YAG crystal. In 2009, Xie et al. generated a passively mode-locked Nd:CLNGG disordered crystal laser with the pulse of 900 fs [4]. Qin et al. demonstrated Nd,Y:CaF_2 disordered crystal laser with pulse duration as short as 103 fs [5]. Ma et al. achieved stable continuous-wave mode-locked pulses as short as 79 fs from Nd:$Ca_3La_2(BO_3)_4$ disordered crystal [6].

$SrAl_{11}O_{19}$ (SRA) crystallizes in the magneto-plumbite structure with the space group $P6_3/mmc$ [7-9]. SRA crystal exhibits an excellent thermal conductivity of 11 W/m·K and high Moh's hardness of 9 [10]. When it is doped with Nd^{3+} ion to form Nd:SRA, Nd^{3+} ion will replace the Sr^{2+} ion and charge compensation is achieved by substituting Mg^{2+} ion for Al^{3+} ion, which causes a complex and disordered lattice field in SRA crystal. In 1997, Verdun et al. reported the optical properties including absorption spectra and fluorescence lifetime of Nd^{3+} -doped $SrAl_{12}O_{19}$ crystal grown by the laser-heated pedestal-growth method [11]. Recently, we demonstrated a diode-pumped Nd:SRA *Q*-switched laser for the first time. A high repetition rate of 201 kHz and a *Q*-switched pulse of 346 ns were obtained, with the peak power of 1.87 W and single pulse energy of 0.65 μJ [12].

In this work, Nd:SRA crystal has been grown by the Czochralski method. The polarized spectral of Nd:SRA crystal were studied. Using 800 nm laser diode as pumping source, the continuous-wave laser operation of Nd:SRA crystal was demonstrated.

2. Crystal growth

Nd:SRA crystal with Nd^{3+} concentration of 5 at.% was grown using the Czochralski method. The MgO, $SrCO_3$, Al_2O_3 and Nd_2O_3 powders with purity of 99.999% were used as starting raw materials. They were dried and weighed according to a definite molar ratio. Due to the incongruent melting behavior, an excess of $SrCO_3$ is required to obtain SRA single phase [13]. After the compounds were thoroughly mixed, they were pressed into pellet and then sintered at 1300 ℃ for 20 h in air atmosphere. The charge was then loaded into an iridium crucible for crystal growth. The growth direction was along the crystalline a-axis with the pulling rate of 1mm/h and rotation rate of 10-20 rpm. High-purity nitrogen gas was introduced in the growth chamber as a protective atmosphere. Fig. 1 shows the as-grown Nd:SRA crystal with the size of Φ28×40 mm^3. The crystal boule is transparent pink color. Some inclusions at the end (Tail) of the boule were observed.

In order to confirm the structure of the as-grow Nd:SRA crystal, room temperature powder X-ray diffraction (XRD, Bruker-D2, Germany) at a scan width of 0.05° with a range 2θ = 10-80° was performed. The XRD patterns of Nd:SRA crystal is displayed in Fig. 2. The diffraction peaks of the sample match well with the SRA standard card (JCPDS 80-1195). The data reveals that the as-grown Nd:SRA crystal possesses a hexagonal system with the space group of $P6_3/mmc$. The cell parameters of Nd:SRA crystal were measured to be a=b=5.5638(3)Å, c=21.98558(5)Å. The Nd^{3+} ions concentration in Nd:SRA crystal was measured with an inductively coupled plasma atomic emission spectrometry (ICP-AES). The segregation coefficient of Nd^{3+} ions in Nd:SRA crystal was calculated to be arround 1.35.

Fig. 1. As-grown single crystal ingot of Nd:SRA.

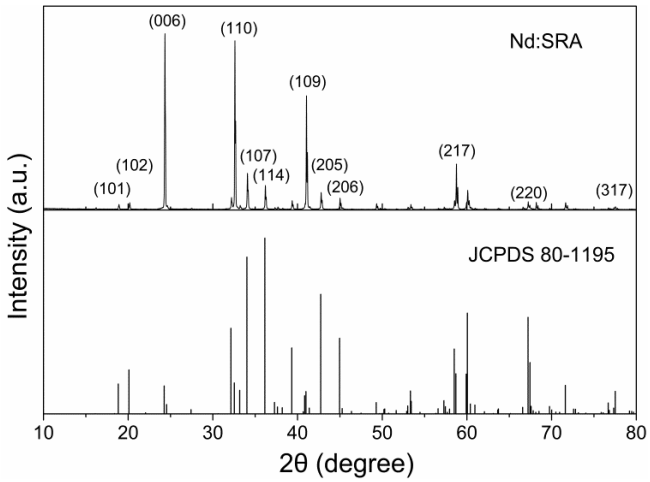

Fig. 2. Room temperature X-ray diffraction pattern of Nd:SRA crystal and standard pattern of SRA.

3. Spectral properties

The crystal sample for spectroscopic measurements was cut from the as-grown Nd:SRA crystal, and the surfaces perpendicular to the < 100 > growth axis were polished. The selected Nd^{3+} dopant concentration has been chosen to avoid strong emission quenching. The polarized absorption spectra were measured with a UV/VIS/NIR spectrophotometer (Model Cary-5000, Varian, USA) at room temperature. The fluorescence spectra and the fluorescence lifetime were recorded with an Edinburg Instrument FLS980 fluorescence spectrometer under 796 nm excitation. All the measurements were taken at room temperature.

Fig. 3 presents the polarized absorption spectra of Nd:SRA crystal in the wavelength region of 300-1000 nm. All the absorption bands corresponding to transitions from the $^4I_{9/2}$ ground state to the various excited states of Nd^{3+} ions are marked. The absorption spectra show strong polarization dependence due to the anisotropy of the crystal, and the absorption cross-section of the σ polarization is much higher than that of the π polarization. The absorption cross sections were calculated to be 2.08×10^{-20} cm^2 at 798 nm for σ polarization and 0.21×10^{-20} cm^2 at 794 nm for π polarization, with full width at half maximum (FWHM) of 10.2 nm and 23.4 nm, respectively. The relatively large FWHM permits high conversion efficiency when pumped by AlGaAs laser diode. Besides, the absorption cross section for σ polarization is comparable with that of $Nd:Ca_{0.7}La_{0.3}Mg_{0.3}Al_{11.7}O_{19}$ (2.18×10^{-20} cm^2 at 792 nm [14]), but is much larger than the value of $Nd:LaMgAl_{11}O_{19}$ (1.7×10^{-20} cm^2 at 795 nm [15]) and $Nd:Sr_{0.7}La_{0.3}Mg_{0.3}Al_{11.7}O_{19}$ (8.6×10^{-21} cm^2 at 792 nm [16]).

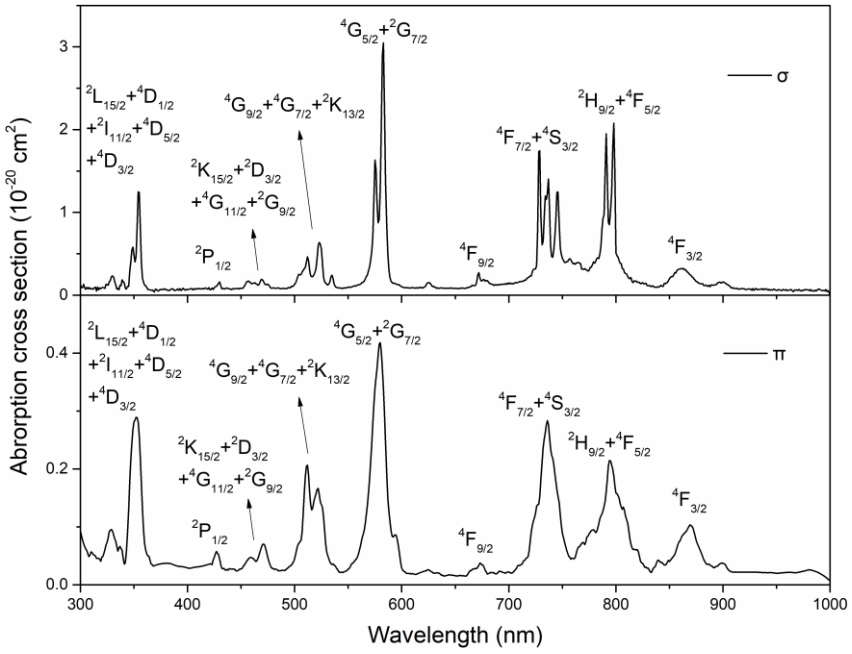

Fig. 3. Polarized absorption spectra of Nd:SRA crystal at room temperature.

The Judd-Ofelt theory [17,18], which is the most popular and useful method for evaluating spectroscopic parameters of rare earth ions in materials, was applied in our paper. The reduced matrix elements used for absorption and emission transitions can be found in references [19] and [20], respectively. The J-O intensity parameters Ω_2, Ω_4 and Ω_6 are listed in Table 1. The effective J-O intensity parameters were calculated by $\Omega= (2\Omega_\sigma+ \Omega_\pi)/3$, and the $\Omega_{2,4,6}$ were obtained to be 0.51×10^{-20} cm^2, 2.08×10^{-20} cm^2, and 2.12×10^{-20} cm^2, respectively. In general, Ω_2 is covalency-dependent parameter related to contravalency of the Nd^{3+} ion sites. Compared with Nd:YAG ($\Omega_{2,4,6}$ = 0.2, 2.7, and 5.0×10^{-20} cm^2 [21]), Nd:SRA has a relatively large Ω_2 value, which indicates that the covalency of Nd:SRA is higher than that of Nd:YAG.

The spontaneous transition rate, branching ratios and the radiative lifetime of $^4F_{3/2}\rightarrow{}^4I_{9/2}$, $^4F_{3/2}\rightarrow{}^4I_{11/2}$, $^4F_{3/2}\rightarrow{}^4I_{13/2}$ and $^4F_{3/2}\rightarrow{}^4I_{15/2}$ transitions of Nd:SRA crystal are given in Table 2. We can see that the branching ratio of the $^4F_{3/2}\rightarrow{}^4I_{9/2}$ transition is smaller than that of the $^4F_{3/2}\rightarrow{}^4I_{11/2}$ transition for σ polarization, but larger than that of the $^4F_{3/2}\rightarrow{}^4I_{11/2}$ transition for π polarization. The radiative lifetime of $^4F_{3/2}$ energy level was calculated to be 552 μs, which is much longer than the value of $Nd:Ca_{0.7}La_{0.3}Mg_{0.3}Al_{11.7}O_{19}$ (364 μs [14]), $Nd:LaMgAl_{11}O_{19}$ (401 μs [15]), $Nd:Sr_{0.7}La_{0.3}Mg_{0.3}Al_{11.7}O_{19}$

(500 μs at 792 nm [16]), Nd:$KGd(WO_4)_2$ (111 μs [22]), Nd:$Bi_4Ge_3O_{12}$ (293 μs [23]), and Nd:$BaBi_2(MoO_4)_4$ (115 μs [24]). The results indicate that Nd:SRA crystal has a higher energy storge ability.

Table 1. The J-O intensity parameters of Nd:SRA crystal.

Intensity parameter	Ω (10^{-20} cm^2)		
	σ-polarization	π-polarization	$\Omega=(2\Omega_\sigma+\Omega_\pi)/3$
Ω_2	0.72	0.10	0.51
Ω_4	2.59	1.07	2.08
Ω_6	2.93	0.51	2.12

Table 2. The spontaneous transition rate, branching ratios and radiative lifetime for different transition levels of Nd:SRA crystal.

Transitions	σ-polarization		π-polarization	
$^4F_{3/2}\rightarrow$	$A_\sigma(S^{-1})$	$\beta_\sigma(\%)$	$A_\pi(S^{-1})$	$\beta_\pi(\%)$
$^4I_{9/2}$	997.12	41.82	363.48	55.13
$^4I_{11/2}$	1153.31	48.37	254.77	38.64
$^4I_{13/2}$	229.22	9.61	40.19	6.10
$^4I_{15/2}$	4.88	0.20	0.84	0.13
Radiative lifetime (μs)	τ_{rad} = 552			

The polarized fluorescence spectra of Nd:SRA crystal in the range of 850-1450 nm was recorded under 796 nm excitation. The stimulated emission cross section can be calculated from the fluorescence spectra using the Füchtbauere Ladenburg (F–L) formula [25]. Fig. 4 presents the stimulated emission cross section for each polarization, and three emission bands are assigned to the transitions from $^4F_{3/2}$ energy level to $^4I_{9/2}$, $^4I_{11/2}$ and $^4I_{13/2}$ energy level, respectively. The emission cross section of the σ polarization is larger than that of the π polarization. The peak emission cross section was calculated to be 3.36×10^{-20} cm^2 for σ polarization and 0.65×10^{-20} cm^2 for π polarization both at 1048.5 nm, respectively, with FWHM of 4.80 and 8.25 nm. The emission cross section of $^4F_{3/2}\rightarrow{}^4I_{11/2}$ transition for σ polarization is smaller than the value of Nd:$Ca_{0.7}La_{0.3}Mg_{0.3}Al_{11.7}O_{19}$ (4.01×10^{-21} cm^2 at 1052 nm [14]) and Nd:$LaMgAl_{11}O_{19}$ (4.08×10^{-20} cm^2 at 1054.5 nm [15]).

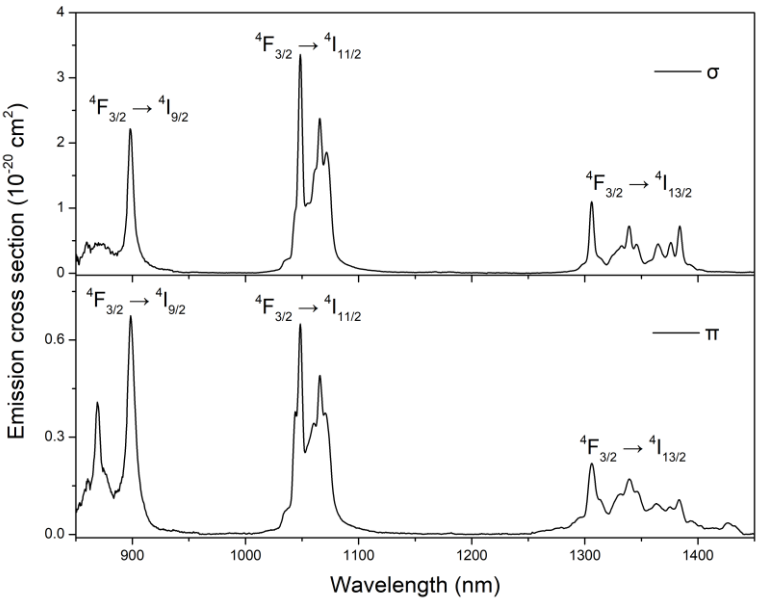

Fig. 4. Polarized emission spectra of Nd:SRA crystal excited by 796 nm at room temperature

Fig. 5 shows the fluorescence decay curve of the $^4F_{3/2}$ multiplet. The decay curve shows a single exponential decaying behavior. The fluorescence lifetime was fitted to be 436 μs, which is much longer than that of Nd:$Ca_{0.7}La_{0.3}Mg_{0.3}Al_{11.7}O_{19}$ (333 μs [14]), Nd:$LaMgAl_{11}O_{19}$ (321 μs [15]), Nd:$Sr_{0.7}La_{0.3}Mg_{0.3}Al_{11.7}O_{19}$ (372 μs [16]), Nd:CaYAlO4 (129 μs [26]), Nd:$GdNbO_4$ (178 μs [27]) and

Nd:YAG (248 μs [28]). According to the radiative lifetime from Table. 2, the luminescent quantum efficiency of the $^4F_{3/2}$ level was calculated to be 79.0% by the equation of $\eta=\tau_f/\tau_{rad}$. The results show that Nd:SRA crystal is a promising gain medium for solid-state laser.

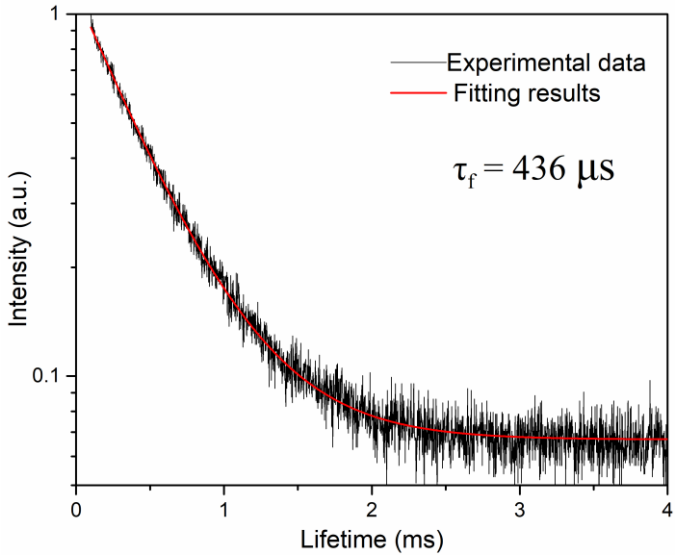

Fig. 5. The fluorescence decay curve of the $^4F_{3/2}$ manifold of Nd:SRA

4. Laser properties

Samples used in the laser experiments were cut along *a* and *c* crystalline axis with dimensions of 3 × 3 × 6 mm^3. The LD-pumped continuous-wave laser performance of Nd:SRA was carried out in a simple plano-plano resonator. The schematic diagram of the setup is the same as in [14]. The pump source was a fiber-coupled 800 nm AlGaAs diode laser with a core diameter of about 200 μm and a numerical aperture of 0.22. Three different output couplers (OCs), with transmissions of 5%, 10% and 15% at 1049 nm, were used in the experiments.

Fig. 6(a) shows the output power as a function of absorbed pump power of a-cut Nd:SRA laser. The threshold absorbed pump powers were 0.04, 0.099 and 0.05W, respectively, for the OCs with transmissions of 5%, 10% and 15%. When the output coupler transmission was 10%, a maximum output of 4.315 W was achieved at the absorbed pump power of 15.41 W, corresponding to an optical-to-optical conversion efficiency of 28.0% and a slope efficiency of 28.8%. The laser spectrum registered at maximum output power is shown in Fig. 6(b) with peak wavelength of about 1049.48 nm.

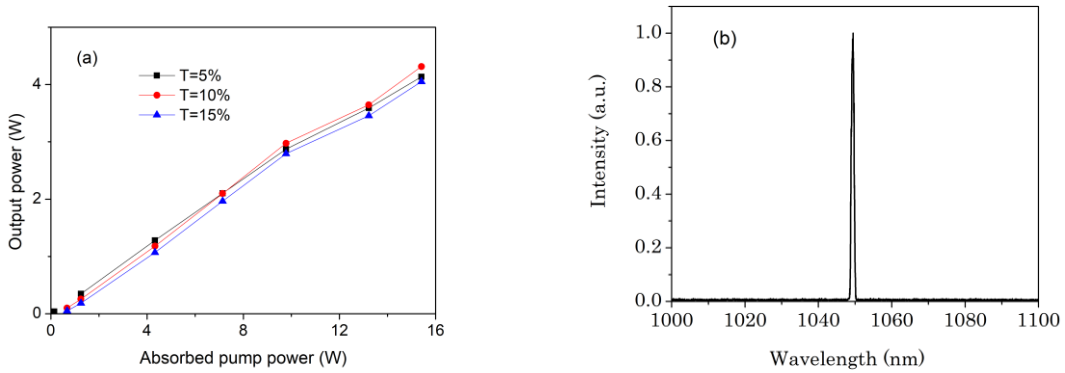

Fig. 6 (a)Output powers versus absorbed pump powers of doped-pumped a-cut Nd:SRA laser and (b) corresponding laser spectrum achieved at maximum output power

The dependence of the output power on the absorption pump power of c-cut Nd:SRA laser is illustrated in Fig. 7(a). Using the output coupler with transmission of 5%, a maximum output power reached about 7.19 W with the threshold of about 0.061 W and the slope efficiency of about 26.8%. Using the output coupler with transmission of 10%, a maximum output power up to 8.25 W was

achieved with the threshold of 0.032 W of absorbed power, which led to a slope efficiency of about 30.5%. Using the output coupler with transmission of 15%, the maximum output power increased to 8.33 W with the threshold of about 0.091 W. The slope efficiency was linearly fitted to be about 31.3% and the corresponding optical-to-optical conversion efficiency was 30.0%. The maximum output power of Nd:RSA is larger than that of Nd:$Ca_{0.7}La_{0.3}Mg_{0.3}Al_{11.7}O_{19}$ (5.40 W [14]), Nd:$LaMgAl_{11}O_{19}$ (1.71 W [15), Nd:$Sr_{0.7}La_{0.3}Mg_{0.3}Al_{11.7}O_{19}$ (6.9 W [16]), but the slope efficiency of Nd:SRA is lower than that of Nd:$Ca_{0.7}La_{0.3}Mg_{0.3}Al_{11.7}O_{19}$ (47.7% [14]), Nd:$LaMgAl_{11}O_{19}$ (40.4% [15), Nd:$Sr_{0.7}La_{0.3}Mg_{0.3}Al_{11.7}O_{19}$ (50% [16]). At maximum output power, the peak wavelength was measured to be 1049.28 nm (see Fig. 7(b)). There was no pump saturation in our experiments, which indicates the output power can be further scaled with high pump power.

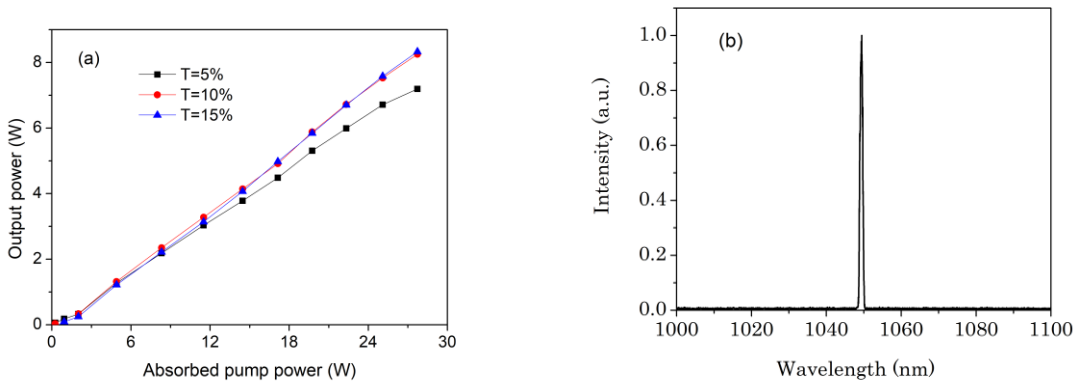

Fig. 7 (a)Output powers versus absorbed pump powers of doped-pumped c-cut Nd:SRA laser and (b) corresponding laser spectrum achieved at maximum output power

5. Conclusions

~~In conclusion,~~ Nd:SRA crystal has been grown from the melt by Czochralski method. The crystal crystallizes in the hexagonal system with space group $P6_3/mmc$. The cell parameters of Nd:SRA crystal were measured to be a=b=5.5638Å, c=21.98558Å. Polarized absorption spectra, polarized fluorescence spectra and fluorescence lifetime were investigated. The peak absorption cross-section was 2.08×10^{-20} cm^2 at 798nm for σ polarization, with the FWHM of 10.18 nm. The effective intensity parameters $\Omega_{2,4,6}$ were obtained to be 0.51×10^{-20} cm^2, 2.08×10^{-20} cm^2, and 2.12×10^{-20} cm^2, respectively. The peak emission cross section was 3.36×10^{-20} cm^2 for σ-polarization at 1048.5 nm, with a FWHM of 4.80 nm. The radiative and fluorescence lifetime are 552 and 436 μs, respectively, resulting in a quantum efficiency of 79.0%. Continuous-wave laser operation of Nd:SRA under 800nm laser diode has been demonstrated. For a-cut sample, the maximum output power of 4.315 W was obtained at an absorbed power of 15.41 W with the T_{OC} = 10%, corresponding to a slope efficiency of 28.8%. For c-cut sample, the maximum output power of 8.33 W was obtained at an absorbed power of 27.73 W with the T_{OC} = 15%, corresponding to a slope efficiency of 31.3%.

Funding

National Natural Science Foundation of China (No. 61621001) and "Qinglan Project" of the Young and Middle-aged Academic Leader of Jiangsu College and University.

Disclosures. The authors declare no conflicts of interest.

References

1. T. J. Kane, W. J. Kozlovshy, and R. I. Byer, "Coherent laser radar at 1.06 μm using Nd:YAG lasers," Opt. Lett. **12**(4), 239-241 (1987).
2. K. Washio, "Neodymium-doped solid-state lasers and their applications to materials processing," Mater. Chem. Phys. 31(1-2), 57-66 (1992)
3. R. Moncorge, B. Chambon, J. Y. Rivoire, N. Garnier, E. Descroix, P. Laporte, H. Guillet, S. Roy, J. Mareschal, D. Pelenc, J. Doury, and P. Farge, "Nd doped crystals for medical laser applications," Opt. Mater. **8**(1-2) 109-119 (1997)
4. G. Q. Xie, D. Y. Tang, W. D. Tan, H. Luo, H. J. Zhang, H. H. Yu, and J. Y. Wang, "Subpicosecond pulse generation from a Nd:CLNGG disordered crystal laser," Opt. Lett. **34**(1), 103-105 (2009)
5. Z. P. Qin, G. Q. Xie, J. Ma, W. Y. Ge, P. Yuan, L. J. Qian, L. B. Su, D. P. Jiang, F. K. Ma, Q. Zhang, Y. X. Cao, and J. Xu, "Generation of 103 fs mode-locked pulses by a gain linewidth-variable Nd,Y:CaF_2 disordered crystal," Opt. Lett. **39**(7), 1737-1739 (2014)

6. J. Ma, Z. B. Pan, H. Q. Cai, H. H. Yu, H. J. Zhang, D. Y Shen, and D. Y. Tang, "Sub-80 femtosecond pulses generation from a diode-pumped mode-locked Nd:$Ca_3La_2(BO_3)_4$ disordered crystal laser," Opt. Lett. **41**(7), 1384-1387 (2016)
7. A. J. Lindop, C. Matthews, D. W. Goodwin, "Refined structure of $Sr_{0.6}Al_2O_3$," Acta Crystallogr. B **31**, 2940-2941 (1975)
8. L. D. Merkle, B. Zandi, R. Moncorge, Y. Guyot, H. R. Verdun and B. Mclntosh, "Spectroscopy and laser operation of Pr,Mg:$SrAl_{12}O_{19}$," J. App. Phys. **79**(4), 1849-1856 (1996)
9. J. Liu, Q. S. Song, D. Z. Li, X. D. Xu, and J. Xu, "Growth and red-orange emission of Sm^{3+} doped $SrAl_{12}O_{19}$ single crystals," Opt. Mater. **101**, 109754 (2020)
10. M. Fechner, F. Reichert, N.-O. Hansen, K. Petermann, G. Huber, "Crystal growth, spectroscopy, and diode pumped laser performance of Pr,Mg:$SrAl_{12}O_{19}$," App. Phys. B **102**, 731-735 (2011)
11. H. R. Verdum, D. E. Wortman, C. A. Morrison, and J. L. Bradshaw, "Optical properties of Nd^{3+} in single crystal $SrAl_{12}O_{19}$," Opt. Mater. **7**. 117-128 (2007)
12. M. F. Zhao, Z. M. Zhang, X. Y. Feng, M. Y. Zong, J. Liu, X. D. Xu, and H. Zhang, "High repetition rate passively *Q*-switched laser on Nd:SRA at 1049 nm with MXene $Ti_3C_2T_x$," Chin. Opt. Lett. **18**(4), 041401 (2020)
13. F. Gantis, T. Y. Chemkova, and Y. P. Udalov, "Sr-Al_2O_3 system," Russ. J. Inorg. Chem., **24**, 260 (1979)
14. Y. X. Pan, B. Liu, J. Liu, Q. S. Song, J. Xu, D. Z. Li, P. Liu, J. Ma, X. D. Xu, H. Lin, J. Xu, and K. Lebbou, "Spectroscopic properties and continuous-wave laser operation of Nd:$Ca_{0.7}La_{0.3}Mg_{0.3}Al_{11.7}O_{19}$," Opt. Mater. Express **10**(5), 1255-1263 (2020)
15. Y. X. Pan, S. D. Zhou, J. W. Wang, B. Xu, J. Liu, Q. S. Song, J. Xu, D. Z. Li, P. Liu, X. D. Xu, and J. Xu, "Growth, spectral properties, and diode-pumped laser operation of a Nd^{3+}-doped $LaMgAl_{11}O_{19}$ crystal," Appl. Opt. **57**(32), 9657-9661 (2018).
16. L. H. Zheng, P. Loiseau, and G. Aka, "Diode-pumped laser operation at 1053 and 900 nm in $Sr_{1-x}La_{x-y}Nd_yMg_xAl_{12-x}O_{19}$ (Nd:ASL) single crystal," Laser Phys. **23**(9), 095802 (2013).
17. B. R. Judd, "Optical absorption intensities of rare-earth ions," Phys. Rev. **127**(3), 750-761 (1962).
18. G. S. Ofelt, "Intensities of crystal spectra of rare- earth ions," J. Chem. Phys. **37**(3), 511-520 (1962).
19. W. T. Carnall, P. R. Fields, and K. Rajnak, "Energy levels in the Trivalent Lanthanide Aqua Ions. I. Pr^{3+}, Nd^{3+}, Pm^{3+}, Sm^{3+}, Dy^{3+}, Ho^{3+}, Er^{3+}, and Tm^{3+}," J. Chem. Phys. **49**(10), 4424-4442 (1968).
20. A. A. Kaminskii, G. Boulon, M. Buoncristiani, B. Di Bartolo, A. Kornienko, and V. Mironov, "Spectroscopy of a new laser garnet $Lu_3Sc_2Ga_3O_{12}$:Nd^{3+}. Intensity luminescence characteristics, stimulated emission, and full set of squared reduced- matrix elements $|\langle \| U^{(t)} \| \rangle|^2$ for Nd^{3+} ions," Phys. Status Solidi (a) **141**(2), 471-494 (1994).
21. W. F. Krupke, "Radiative transition probabilities within $^4F_3$ ground configuration of Nd-YAG," IEEE J. Quantum Electron. **7**(4), 153 (`1971)
22. Y. J. Chen, Y. F. Lim X. H. Gong, Q. G. Tan, J. Zhuang, Z. D. Luo, and Y. D. Huang, "Polarized spectroscopic properties of Nd^{3+}-doped $KGd(WO_4)_2$ single crystal," J. Lumin. **126**, 653-660 (2007)
23. N. Li, Y. Y. Xue, D. H. Wang, B. Liu, C. Guo, Q. S. Song, X. D. Xu, J. F. Liu, D. Z. Li, J. Xu, Z. A. Xu, and J. Y. Xu, "Optical properties of Nd:$Bi_4Ge_3O_{12}$ crystals grown by the micro-pulling-down method," J. Lumin. **206**, 412-416 (2019)
24. A. V. Lebedev, S. A. Avanesov, V. A. Klimenko, L. V. Vasileva, and A. Hammoud, "Growth and spectroscopic studies of Nd^{3+}-doped $BaBi_2(MoO_4)_4$ crystal," **103**, 109901 (2020)
25. B. Aull and H. Jenssen, "Vibronic interactions in Nd:YAG resulting in nonreciprocity of absorption and stimulated emission cross sections," IEEE J. Quantum Electron. **18**, 925–930 (1982).
26. D.Z Li, X.D. Xu, S.S. Cheng, D.H. Zhou, F. Wu, Z.W. Zhao, C.T. Xia, J. Xu, H.M. Zhu, and X.Y. Chen, "Polarized spectral properties of Nd^{3+} ions in $CaYAlO_4$ crystal," Appl. Phys. B **101**, 199-205 (2010)
27. S.J. Ding, F. Peng, Q.L. Zhang, J.Q. Luo, W.P. Liu, D.L. Sun, R.Q. Dou, J.Y. Gao, G.H. Sun, and M.J. Cheng, "Crystal growth, spectral properties, and continuous wave laser operation of Nd:$GdNbO_4$," J. Alloys Compd. **693**, 339-343 (2017)
28. S. Singh, R.G. Smith, and L.G. Van Uitert, "Stimulated-emission cross section and fluorescent quantum efficiency of Nd^{3+} in yttrium aluminum garnet at room temperature," Phys. Rev. B **10**, 2566-2572 (1974)